J Membrane Biol (2010) 238:63–68
DOI 10.1007/s00232-010-9319-5

Ca^{2+}-Induced Effect on Mechanical Properties of Sulfatide-Incorporated Vesicles

Jin-Won Park

Received: 13 September 2010 / Accepted: 3 November 2010 / Published online: 19 November 2010

Abstract The Ca^{2+}-induced effect on the nanomechanical properties of vesicles prepared at a different ratio of dipalmitoylphosphatidylcholine (DPPC)/sulfatide was studied using atomic force microscope (AFM) on a mica surface. Vesicles were prepared by extrusion and adsorbed on the mica surface. The forces, measured between an AFM tip and the vesicle, showed that the breakthrough of the tip into the vesicles occurred two times. Force data prior to the first breakthrough were fitted well with the Hertzian model to estimate Young's modulus and bending modulus of the vesicles. Sulfatide incorporation led to a decrease of around 90% in Young's modulus and bending modulus of the vesicles due to the hydration of the headgroups, while the addition of Ca^{2+} induced dehydration to recover the properties. The change of the physical properties seems to be attributed to the headgroup packing order of the vesicles, which is determined by the interference with the hydration shell.

Keywords Biophysical techniques in membrane research · Biophysics · Measurement · Membrane assembly · Membrane biophysics

Introduction

Sulfatides (galactosylceramidesulfates) are negatively charged glycosphingolipids that are minor constituents of most eukaryotic membranes but major in the nervous system and especially important for brain myelin membranes (Norton and Autilio 1966). In many cells, sulfatides have been found to function as receptors for neurotransmitters, opiates, endorphins and a heat shock protein, Hsp70 (Loh et al. 1974; Craves et al. 1980; Mamelk and Lingwood 2001; Mamelk et al. 2001; Yandrasitz et al. 2001; Harada et al. 2007). It is also documented that sulfatides control insulin secretion by modulation of ATP-sensitive K^+-channel activity and Ca^{2+}-dependent exocytosis in rat pancreatic ß-cells (Buschard et al. 2002). In the myelin membranes, sulfatides participate in contact formation between bilayers through interaction with galactoylceramide, a neutral glycosphingolipid (Boggs et al. 2000, 2004; Hakomori 2004). This interaction is important for the stability of the myelin in the central nervous system, and the myelin membranes are also highly enriched in both galactosylceramide and cholesterol (Boggs et al. 2000, 2004). It is becoming increasingly evident that glycosphingolipids take part in cell–cell interactions, possibly through defined membrane regions called "glycosignaling domains" (Hakomori 2004). Therefore, understanding the physical behavior of sulfatides seems to play an important role in biological membranes.

It is generally accepted that the fusion involved in endocytosis requires dehydration of bilayer headgroups and destabilization of the bilayer structure (Wu and Li 1999). Furthermore, the stability depends on the physical properties of the membranes (Manojlovic et al. 2008). In previous studies, work on the membrane properties of sulfatides has often been conducted on biological mixtures of sulfatides with a variety of acyl chains of different lengths, degrees of hydroxylation and concentrations of divalent cations (Weerachatyanukul et al. 2007; Boggs et al. 1988; Menikh et al. 1997). The effect of sulfatide incorporation on the physical properties of the membranes

J.-W. Park (✉)
Department of Chemical Engineering, College of Engineering, Seoul National University of Science and Technology, 172 Gongreung 2-dong, Nowon-gu, Seoul 139-743, South Korea
e-mail: jwpark@seoultech.ac.kr

made with dipalmitoylphosphatidylcholines (DPPCs) has also been found. The mechanical properties of the membranes were reduced by the membrane structure interference caused by hydration of the sulfatides (Park 2010). Therefore, it is interesting to examine the effect that Ca^{2+} has on the mechanical properties of the membranes because Ca^{2+} is known as a physiological stimulus of fusion, especially dehydration.

Atomic force microscopy (AFM) has been widely used for measurements of forces of interaction between the AFM probe and the surface, providing information about the physical properties of the sample surface (Fang et al. 2000; Beech et al. 2002; Engler et al. 2004). On approach of the AFM probe tip to the sample surface, repulsive forces can be acquired, such as electrostatics, salvation, hydration and compression-related steric forces. The retraction force data often show a hysteresis referred to as an "adhesion pull-off," which can be used to evaluate adhesion forces. Theoretical models have been developed for the analysis of forces between two solid surfaces (Cappella and Dietler 1999; Senden et al. 1994; Biggs 1995; van der Vegte and Hadziioannou 1997; Dimitriadis et al. 2002). In this work, we investigated the change in the mechanical properties of sulfatide-incorporated DPPC vesicles caused by Ca^{2+}.

Experiments

DPPC and sulfatides were purchased from Avanti Polar Lipids (Alabaster, AL) and used without further purification. Lipids were dissolved in chloroform and methanol (70:30) with a desired composition of sulfatides in the mixture of the lipids. Chloroform and methanol were subsequently removed using a dry stream of nitrogen. The lipid film was dried overnight at low pressure to remove any trace impurities of the organic solvent. Films were immersed in a buffer solution containing 10 mM HEPES, 50 mM KCl and 1 mM NaN_3 at pH 7. The lipid suspension was kept for at least 1 h at 10°C above the gel–fluid transition temperature. During this period the suspension was vortexed several times. Large unilamellar vesicles were made by extruding the suspension through two stacked 100-nm-pore size polycarbonate filters. For the composition, 0, 5, 10, 15 and 20 mol% were selected because it was found that the sulfatides were stably mixed with DPPC in their bilayer configuration up to 20 mol% (Cestaro et al. 1981). Dynamic light scattering was used to measure the diameter of the vesicles (ELS-8000; Otsuka, Tokyo, Japan). The diameter of all vesicles was approximately 150 ± 20 nm.

AFM measurements were made at 25°C using an optical lever microscope equipped with a liquid cell (Nanoscope v5.12; Veeco, Santa Barbara, CA). Contact-mode topographic images were taken in the constant-deflection mode using commercial cantilevers with a typical radius of curvature of 20 nm and spring constants of 0.2 N/m. Mica was placed on the AFM scanner. The AFM cantilever was mounted onto a liquid cell and carefully lowered onto the O-ring, sealing it between the cell and the mica. After the mica was brought close to the AFM cantilever tip, the vesicle solution was injected into the fluid cell. The vesicle solution was allowed to incubate on mica at room temperature for 1 h. Excess vesicles were removed by flushing the fluid cell with the buffer solution. Force curves were obtained on and around the vesicles. However, only the force curves with two jump-in points and the highest onset point were accepted for further analysis. Force curves with two jump-on points correspond to measurements obtained directly on the vesicle and represent the interaction between the tip and the vesicles. After the force measurements at the buffer solution used for the vesicle preparation, the other force measurements were performed at the other buffer solution. The other buffer, containing 10 mM $CaCl_2$, 10 mM HEPES, 50 mM KCl and 1 mM NaN_3 at pH 7, was added into the cell so that the vesicle preparation buffer was replaced. After the replacement, force measurements were made under conditions identical to the previous measurements.

Approaching force distance data was fitted to the Hertzian contact model, assuming a spherical shape for the tip (Laney et al. 1997; Radmacher et al. 1994). The indentation from the difference between the cantilever distance $z - z_0$ and cantilever deflection $d - d_0$ is described in the equation.

$$|z - z_0| - (d - d_0) = \delta = A(d - d_0)^{\frac{2}{3}} = 0.825\left[\frac{k^2\left(R_{\text{tip}} + R_{\text{ves}}\right)\left(1 - v_{\text{ves}}^2\right)^2}{E_{\text{ves}}^2 R_{\text{tip}} R_{\text{ves}}}\right]^{\frac{1}{3}}(d - d_0)^{\frac{2}{3}} \quad (1)$$

where δ is the indentation; E_{ves} is the Young's modulus of the vesicle; R_{tip} and R_{ves} are the radius of the tip and vesicle, respectively; v_{ves} is the Poisson ratio of the vesicle; and k is the cantilever spring constant. The vesicle radius is taken to be equal to $z_0/2$. Experimental data can be fitted to the equation with two fit parameters, A and z_0. In general, the fitted z_0 value was found to be consistent with the visually examined contact point. Thus, z_0 is determined by the onset point of the repulsive force. E_{ves} is then computed from A (obtained by least square fitting). Only data with indentation less than 10 nm were used, to ensure elastic behavior (Laney et al. 1997). Bending modulus, k_c, is deducted from Young's modulus based on the equation

$$k_c = \frac{E_{\text{ves}} h^3}{12\left(1 - v_{\text{ves}}^2\right)} \quad (2)$$

where h is the bilayer thickness.

Results and Discussion

In nanometer-scale morphology, no fusion after the addition of $CaCl_2$ was found. No significant change in morphology was observed after the addition, although $CaCl_2$ is known to be a fusogenic agent. Therefore, it was inferred that $CaCl_2$ might not be a fusogenic agent all of the time. In this research, a study was conducted to find out the $CaCl_2$-induced effect on the mechanical properties based on understanding the interaction between $CaCl_2$ and biological membranes. The image before lipid vesicle adsorption is presented in Fig. 1a. In Fig. 1a, maximum step height is <1 nm and the cross section width of most morphological bumps is almost flat. The morphology after adsorption is presented in Fig. 1b. Step height reaches almost 10 nm and the cross section width of most bumps is around 190 ± 60 nm. Addition of $CaCl_2$ did not cause a significant change in either image.

At the approaching force curve, a wealth of stepwise mechanical deformation events was observed on the lipid vesicles. Figure 2a shows a deflection vs. z position plot on vesicles made with 100% DPPC. Figure 2b is a force vs. distance curve based on the data from Fig. 2a. Curves presented in Fig. 2 have four regions, as labeled. In region 1, the noncontact region, the tip is far away from the vesicle and the force between the tip and the vesicle is zero. Region 2 illustrates the elastic deformation of the vesicle under tip compression and, therefore, can be used to calculate Young's modulus. In region 3, further tip compression was found after the tip penetrated the vesicle's top bilayer. Region 4 corresponds to the cantilever deflection when it is in contact with the hard mica substrate after penetrating through the vesicle's bottom bilayer. In theory, the slope of region 4 should be 1.0 because the deflection of the cantilever is identical to the z direction movement of the sample on the hard surface (Weisenhorn et al. 1993). Based on the fitted data, a slope of 0.992 was obtained. The two jump-in points during the rise of the steric repulsion reflect the tip penetrating the upper and lower portions of each vesicle, respectively (Liang et al. 2004). The onset of a repulsive regime on the bilayer found at around 6 nm suggests that there is no bilayer adsorbed

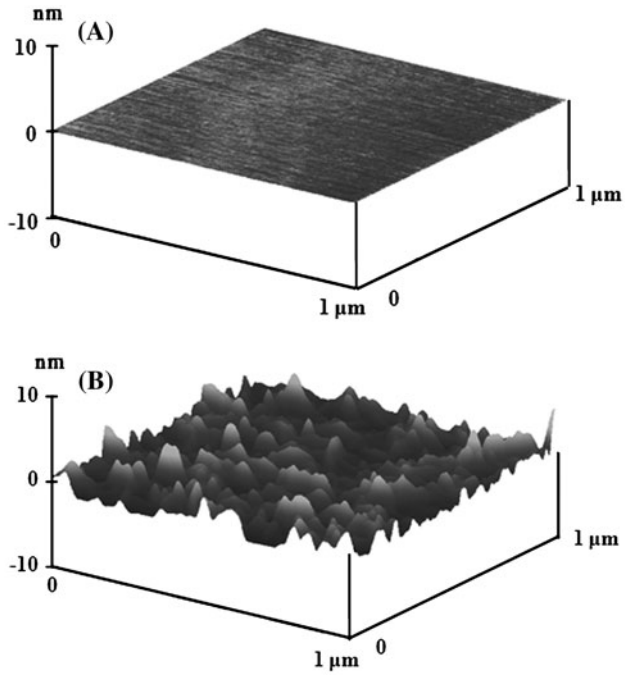

Fig. 1 AFM images **a** before lipid vesicle adsorption and **b** after lipid vesicle adsorption

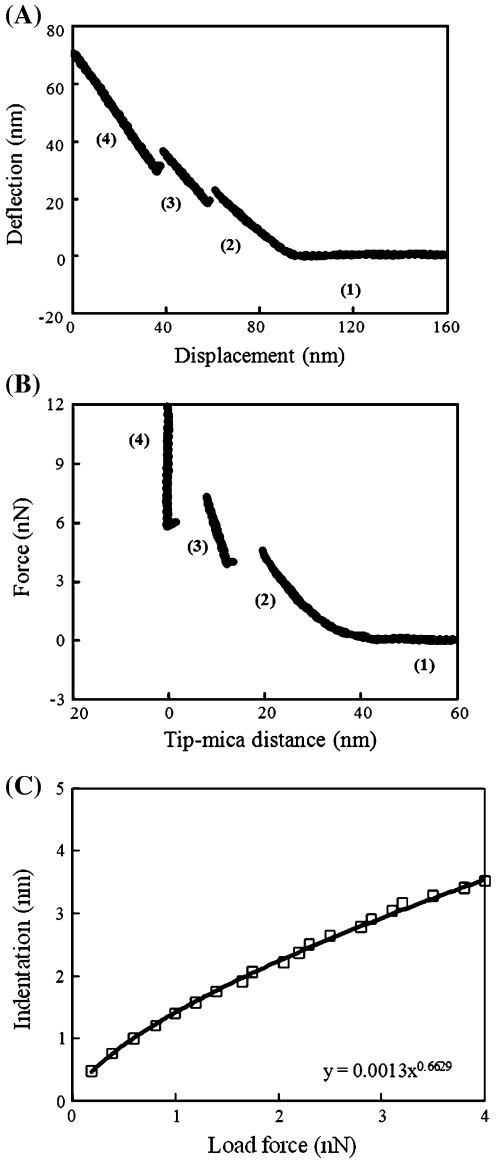

Fig. 2 **a** Deflection vs. z position plot on vesicle made with 100% DPPC, **b** force vs. distance curve based on the data from **a**, **c** indentation vs. load force based on the data from **a** region (2)

on the tip and force measurements were made on mica. This result is also consistent with the force curves made with a clear tip in pure water and with the tip having been in the vesicle solution for several hours.

The slope of a force curve describes the elastic properties of a sample (Laney et al. 1997; Weisenhorn et al. 1993). The slope values of the first repulsive region 2 and second repulsive region 3 before and after the first breakthrough point for different molar ratio sulfatide/DPPC systems and the addition of $CaCl_2$ are listed separately in Table 1. The experimental results shown are average values, and the range of the results is <3%. The slope values for the pure DPPC vesicles of the two repulsive force regimes are 0.7 and 3.6 N/m, respectively. The values lay in the range of 0.63–0.67 and 3.2–3.4 N/m for the sulfatide/DPPC vesicles, which is lower than those for the pure DPPC vesicles. However, the addition of $CaCl_2$ led to an increase in the values close to the vesicles made with 100% DPPC. By fitting experimental data (regions 2 and 3) with the Hertzian contact model $\delta = AF^b$ (where F is loading force), the exponent b was estimated to be 0.663 for region 2 and 0.902 for region 3. From the poor fit in region 3, it was found that the Hertzian model severely fails in region 3. Although the Hertzian model describes the contact between two solid bodies on the basis of continuum elasticity theory without adhesion force (Radmacher et al. 1994), the good fit in region 2 suggests that the Hertzian model may also be applicable to the elastic deformation between the tip and the vesicle within the limit of small indentation. Therefore, all subsequent calculations for determining the nanomechanical properties of the vesicle surfaces were made with the data in region 2 based on the Hertzian model. Figure 2c is the indentation vs. load force based on the data from Fig. 2a, region 2. It shows that there is good agreement between the experimental data and the Hertzian model.

Young's modulus and bending modulus (k_c) of the tested vesicles were evaluated using Eqs. 1 and 2 with bilayer thickness (h) 5 nm. For the bilayer thickness, it may be necessary to consider the structures of DPPC and sulfatide. DPPC has two carbon 16 tailgroups, while the sulfatide has two tailgroups that are carbon 16 and carbon 24. DPPC and sulfatide are mixed well each other, and the majority of the vesicle component is DPPC. Additionally, since there is only one carbon 24 tailgroup in the sulfatide structure, it is not able to form its own domain. Therefore, it is claimed that the incorporation of sulfatide may not induce any change in the thickness of vesicles. It is noted that the value of Young's modulus is slightly affected by the value of Poisson's ratio (e.g., a 10% deviation of Poisson's ratio from 0.5 to 0.45 causes a 6% increase of Young's modulus). In contrast, the bending modulus would not be affected by Poisson's ratio variation. The bending modulus of vesicles decreased with sulfatide incorporation, while the addition of $CaCl_2$ led to an increase in the values close to the vesicles made with 100% DPPC. This observation is similar to the behavior of the slopes described above. The values are reported in Table 2.

Table 2 lists the Young's modulus and bending modulus of DPPC/sulfatide systems with different molar ratios and $CaCl_2$ effects calculated based on AFM approaching force curves. Compared with pure DPPC, Young's modulus and bending modulus of the sulfatide-incorporated vesicles were found to decrease significantly. Young's modulus and bending modulus of the pure DPPC vesicles were 81×10^6 Pa and 11.3×10^{-19} J, respectively, which are in good agreement with previous data (Lee et al. 2001). The change in elastic properties seems to be caused by the sulfatide incorporation. The incorporation seems to lead to the change in bilayer packing geometrical structures. The sulfogalactosyl headgroup of sulfatide forms a hydration shell, which disturbs the packing order of the lipid layer (Westerlund and Slotte 2009). The sulfatide headgroup has a larger surface area (75 $Å^2$) compared to the DPPC headgroup (50 $Å^2$), and the sulfatide headgroup is anionic while the DPPC headgroup is zwitterionic (Cevc and Marsh 1987). The hydration shell apparently interferes with the attractive interactions, involving intermolecular hydrogen bonding and van der Waals bonding between DPPC headgroups. This interference is in good agreement

Table 1 Slope of the repulsive forces on sulfatide-incorporated DPPC liposomes

	Sample DPPC:sulfatide molar ratio				
	100:0	95:5	90:10	85:15	80:20
Slope of 1st repulsive force (N/m)					
Without $CaCl_2$	0.7	0.67	0.65	0.64	0.63
With $CaCl_2$	0.7	0.7	0.7	0.7	0.7
Slope of 2nd repulsive force (N/m)					
Without $CaCl_2$	3.6	3.4	3.3	3.3	3.2
With $CaCl_2$	3.6	3.6	3.6	3.6	3.6

Table 2 Comparison of Young's modulus (E) and bending modulus (k_c) of liposomes with different sulfatide and DPPC ratios

	Sample DPPC:sulfatide molar ratio				
	100:0	95:5	90:10	85:15	80:20
$E_{ves} \times 10^6$ (Pa)					
Without $CaCl_2$	81	78	76	74	73
With $CaCl_2$	81	81	81	81	81
$k_c \times 10^{-19}$ (J)					
Without $CaCl_2$	11.3	10.8	10.5	10.3	10.1
With $CaCl_2$	11.3	11.3	11.3	11.3	11.3

with previous research. Disappearance of DPPC pretransition and broadening of the transition peak, caused by sulfatide, were found (Pedersen et al. 1999). Young's modulus and the bending modulus of vesicles containing sulfatide were decreased to around 90% of those with pure DPPC.

However, it was not predicted that the addition of $CaCl_2$ provided properties identical to those of the pure DPPC vesicles. The addition led to recovery of the mechanical properties to those of the pure DPPC vesicles. This observation appears to be related to the role of Ca^{2+}, which was found to induce dehydration around the headgroups (Wu and Li 1999). Therefore, addition of Ca^{2+} might reduce the interference with the attractive interactions so that the packing order seems to be recovered. From this study, it is found that the physical properties of the vesicle components may be the most important when determining whether the fusion event occurs or not. In fact, it may not be described generally that Ca^{2+} is a fusogenic agent for the vesicles.

Conclusion

In this study, Young's modulus (E) and the bending modulus (k_c) for large unilamellar vesicles on a substrate were quantified by analyzing AFM approach force curves based on the Hertzian model. It was found that Young's modulus and the bending modulus decreased by around 90% after sulfatide incorporation into pure DPPC. However, the addition of $CaCl_2$ to 10 mM concentration led to recovery of the mechanical properties to those of pure DPPC vesicles. The change of the physical properties seems to be attributed to the headgroup packing order of the vesicles, which is determined by the interference with the hydration shell.

Acknowledgments This research was supported by the Basic Science Research Program through the National Research Foundation of Korea funded by the Ministry of Education, Science and Technology (2010-0010097). We thank all of the members of the Department of Chemical Engineering at Seoul National University of Science and Technology for help and valuable discussions. We thank Prof. D. J. Ahn, Dr. G. S. Lee, Mr. H. Choi and Mr. C. S. Choi at Korea University for valuable help.

References

Beech IB, Smith JR, Steele AA, Penegar I, Campbell SA (2002) The use of atomic force microscopy for studying interactions of bacterial biofilms with surfaces. Colloids Surf B Biointerfaces 23:231–247

Biggs S (1995) Steric and bridging forces between surfaces fearing adsorbed polymer—an atomic-force microscopy study. Langmuir 11:156–162

Boggs JM, Koshy KM, Rangaraj G (1988) Influence of structural modifications on the phase-behavior of semi-synthetic cerebroside sulfate. Biochim Biophys Acta 938:361–372

Boggs JM, Menikh A, Rangaraj G (2000) Trans interactions between galactosylceramide and cerebroside sulfate across apposed bilayers. Biophys J 78:874–885

Boggs JM, Wang H, Gao W, Arvanitis DN, Gong Y, Min W (2004) A glycosynapse in myelin? Glycoconj J 21:97–110

Buschard K, Høy M, Bokvist K, Olsen HL, Madsbad S, Fredman P, Gromada J (2002) Sulfatide controls insulin secretion by modulation of ATP-sensitive K^+-channel activity and Ca^{2+}-dependent exocytosis in rat pancreatic beta-cells. Diabetes 51:2514–2521

Cappella B, Dietler G (1999) Force–distance curves by atomic force microscopy. Surf Sci Rep 34:1–104

Cestaro B, Cervato G, di Silvestro G (1981) Thermotropic behavior of dipalmitoylphosphatidylcholine-sulfatide liposomes. Ital J Biochem 30:429–436

Cevc G, Marsh D (1987) Phospholipid bilayers: physical principles and methods. Wiley, New York

Craves FB, Zalc B, Leybin L, Baumann N, Loh HH (1980) Antibodies to cerebroside sulfate inhibit the effects of morphine and beta-endorphin. Science 207:75–76

Dimitriadis EK, Horkay F, Maresca J, Kachar B, Chadwick RS (2002) Determination of elastic moduli of thin layers of soft material using the atomic force microscope. Biophys J 82:2798–2810

Engler AJ, Richert L, Wong JY, Picart C, Discher DE (2004) Surface probe measurements of the elasticity of sectioned tissue, thin gels and polyelectrolyte multilayer films: correlations between substrate stiffness and cell adhesion. Surf Sci 570:142–154

Fang HHP, Chan K-Y, Xu L-C (2000) Quantification of bacterial adhesion forces using atomic force microscopy (AFM). J Microbiol Methods 40:89–97

Hakomori S (2004) Carbohydrate-to-carbohydrate interaction, through glycosynapse, as a basis of cell recognition and membrane organization. Glycoconj J 21:125–137

Harada Y, Sato C, Kitajima K (2007) Complex formation of 70-kDa heat shock protein with acidic glycolipids and phospholipids. Biochem Biophys Res Commun 353:655–660

Laney DE, Garcia RA, Parsons SM, Hansma HG (1997) Changes in the elastic properties of cholinergic synaptic vesicles as measured by atomic force microscopy. Biophys J 72:806–813

Lee C-H, Lin W-C, Wang JP (2001) All-optical measurements of the bending rigidity of lipid-vesicle membranes across structural phase transitions. Phys Rev E 64:020910(R)

Liang X, Mao G, Ng KYS (2004) Probing small unilamellar EggPC vesicles on mica surface by atomic force microscopy. Colloids Surf B Biointerfaces 34:41–51

Loh HH, Cho TM, Wu YC, Way EL (1974) Stereospecific binding of narcotics to brain cerebrosides. Life Sci 14:2231–2245

Mamelk D, Lingwood C (2001) The ATPase domain of hsp70 possesses a unique binding specificity for 3′-sulfogalactolipids. J Biol Chem 276:449–456

Mamelk D, Mylvaganam M, Whetstone H, Hartmann E, Lennarz W, Wyrick PB, Raulston J, Han H, Hoffman P, Lingwood CA (2001) Hsp70 s contain a specific sulfogalactolipid binding site. Differential aglycone influence on sulfogalactosyl ceramide binding by recombinant prokaryotic anti eukaryotic Hsp70 family members. Biochemistry 40:3572–3582

Manojlovic V, Winkler K, Bunjes V, Neub A, Schubert R, Bugarski B, Leneweit G (2008) Membrane interactions of ternary phospholipid/cholesterol bilayers and encapsulation efficiencies of a RIP II protein. Colloids Surf B Biointerfaces 64:284–296

Menikh A, Nyholm PG, Boggs JM (1997) Characterization of the interaction of Ca^{2+} with hydroxy and non-hydroxy fatty acid species of cerebroside sulfate by Fourier transform infrared

spectroscopy and molecular modeling. Biochemistry 36:3438–3447

Norton WT, Autilio LA (1966) Lipid composition of purified bovine brain myelin. J Neurochem 13:213–222

Park J-W (2010) Sulfatide incorporation effect on mechanical properties of vesicles. Colloids Surf B Biointerfaces 80:59–62

Pedersen TB, Frokjaer S, Mouritsen OG, Jörgensen K (1999) Phase behavior and lipid-membrane structure of phospholipids–glycosphingolipid liposomes and the thermal unfolding of insulin. J Liposome Res 9:261–274

Radmacher M, Fritz M, Kacher CM, Walters DA, Hansma PK (1994) Imaging adhesion forces and elasticity of lysozyme adsorbed on mica with the atomic-force microscope. Langmuir 10:3809–3814

Senden TJ, Drummond CJ, Kékicheff P (1994) Atomic-force microscopy—imaging with electrical double-layer interactions. Langmuir 10:358–362

van der Vegte EW, Hadziioannou G (1997) Scanning force microscopy with chemical specificity: an extensive study of chemically specific tip–surface interactions and the chemical imaging of surface functional groups. Langmuir 13:4357–4368

Weerachatyanukul W, Probodh I, Kongmanas K, Tanphaichitr N, Johnston LJ (2007) Visualizing the localization of sulfoglycolipids in lipid raft domains in model membranes and sperm membrane extracts. Biochim Biophys Acta 1768:299–310

Weisenhorn AL, Khorsandi M, Kasas S, Gotzos V, Butt H-J (1993) Deformation and height anomaly of soft surfaces studied with an AFM. Nanotechnology 4:106–113

Westerlund B, Slotte JP (2009) How the molecular features of glycosphingolipids affect domain formation in fluid membranes. Biophys Biochim Acta 1788:194–201

Wu X, Li Q-T (1999) Ca^{2+}-induced fusion of sulfatide-containing phosphatidylethanolamine small unilamellar vesicles. J Lipid Res 40:1254–1262

Yandrasitz JR, Cohn RM, Masley B, DelRowe D (2001) Evaluation of the binding of serotonin by isolated CNS acidic lipids. Neurochem Res 5:465–477